Agriculture, Ecosystems and Environment 339 (2022) 108124

Contents lists available at ScienceDirect

Agriculture, Ecosystems and Environment

journal homepage: www.elsevier.com/locate/agee

Assessing almond response to irrigation and soil management practices using vegetation indexes time-series and plant water status measurements

L. González-Gómez [a], D.S. Intrigliolo [b], J.S. Rubio-Asensio [a], I. Buesa [c,d], J.M. Ramírez-Cuesta [b,*]

[a] Departamento de Riego, Centro de Edafología y Biología Aplicada del Segura, Consejo Superior de Investigaciones Científicas (CEBAS-CSIC), Spain
[b] Department of Ecology, Desertification Research Centre (CIDE-CSIC-UV-GV), Moncada, Valencia 46113, Spain
[c] Centro para el Desarrollo Agricultura Sostenible, Instituto Valenciano de Investigaciones Agrarias (CDAS-IVIA), Moncada, Valencia 46113, Spain
[d] Universidad de las Islas Baleares (UIB), Departamento de Biología, Ctra. Valldemossa km 7.5, Palma, Balearic Islands E-07122, Spain

ARTICLE INFO

Keywords:
Precision agriculture
Remote sensing, sustainable agriculture
Sentinel-2
Vegetation cover
Vegetation index

ABSTRACT

Current water scarcity scenario has led to the implementation of sustainable agricultural practices intended to improve water use efficiency. The present work evaluates during three agricultural campaigns (2018–2020) the response of a young almond orchard to two management practices in terms by combining remote sensing indexes (Normalized Difference Vegetation Index, NDVI; and Soil Adjusted Vegetation Indexes, SAVI) and physiological/morphological measurement (stem water potential, Ψ_{stem}; trunk perimeter and canopy diameter). The management practices included (i) sustained deficit irrigation and (ii) soil management. Severe deficit irrigation resulted in lower vegetation indexes (VI) values, Ψ_{stem} and tree dimensions (13 %, 23 % and 14 % lower, respectively) than those obtained for full irrigation strategy; whereas moderate deficit irrigation did not affect any of the parameters analysed. The presence of vegetation cover in the inter-row resulted in a VI_s increase (19–42 %) and in lower tree dimensions (reductions of 7–8 % for trunk perimeter and 0.34–0.37 m for canopy diameter) when compared to bare soil treatment, but did not have any influence on Ψ_{stem}. The present study proves the suitability of remote sensing and physiological measurements for assessing almond response to the different management practices.

1. Introduction

Current climate change scenario and projected world population growing are leading to the adoption of sustainable management practices (SMP) in agriculture intended for increasing food production, while making a more efficient use of water and soil resources (Almagro et al., 2016; Delgado et al., 2013; Eekhout and de Vente, 2019). These SMP can apply to any component of the Soil-Plant-Atmosphere (SPA) continuum. Thus, specifically at soil level, several practices have been proposed for managing organic carbon and nutrients in soil, optimizing soil physical conditions and soil biological processes and minimizing soil erosion from agricultural land (Powlson et al., 2011). At plant level, most SMP are aimed at diversifying crops (crop rotation, mixed cropping and inter-cropping); irrigation and water management (e.g. deficit irrigation strategies, DI; and micro-drippers); using improved varieties (e.g. more tolerant to drought and pests, early maturity crops and short duration varieties); rescheduling planting calendars; and using organic and bio-fertilizers (Wezel et al., 2014).

The Mediterranean basin is characterized by a shortage of rainfall and water resources, so the adoption of SMP is essential in the management of agricultural systems. In this context, the cultivation of almonds in this area requires the implementation of agricultural practices that improve efficiency in the use of water and have a low environmental impact. Although the almond tree is considered a drought-tolerant specie, the availability of water and how it is applied and distributed is a fundamental factor in its development and yield (Goldhamer and Fereres, 2017; Gutiérrez-Gordillo et al., 2020). Deficit irrigation strategies and precision irrigation can help improve water resource management by improving water use efficiency and maintaining an adequate crop yield (González-Dugo et al., 2020; Girona et al., 2005). These strategies are based on applying water below the evapotranspiration requirements (Fereres and Soriano, 2007). Two of the most worldwide used DI strategies are sustained deficit irrigation (SDI) consisting in applying at certain water deficit during the entire growing season; and regulated deficit irrigation (RDI), based on concentrating the water stress imposition only during certain

* Corresponding author.
E-mail address: ramirezcuesta.jm@gmail.com (J.M. Ramírez-Cuesta).

https://doi.org/10.1016/j.agee.2022.108124
Received 15 March 2022; Received in revised form 21 June 2022; Accepted 3 August 2022
Available online 18 August 2022

phenological periods (Fereres and Soriano, 2007). The latter strategy is based on reducing the water supply at certain phenological stages where fruit development and growth are less affected, leading to improvements in water use efficiency and/or fruit quality compared to SDI. In almond orchards, the lower sensitivity stage to water stress is during the kernel-filling period (Girona et al., 2005). Moreover, RDI strategies that deliberately alter soil moisture by watering only part of the rootzone enhance crop responses to soil water deficit compared with conventional deficit irrigated plants receiving the same water supply (Egea et al., 2011).

In current agricultural systems, the introduction of vegetation covers (VC) growing in the inter-row of woody orchards is an important global strategy to reduce soil erosion, runoff and nutrients loss (Liu et al., 2021; Repullo-Ruibérriz de Torres et al., 2021). Moreover, VC increases the organic matter and the biological activity of the soil, improving its structure and water retention capacity (Lal, 2013; Milgroom et al., 2007). Numerous studies analysed the positive effects triggered by the introduction of inter-row VC in almond orchards (Abbasi Surki et al., 2020; Almagro et al., 2016; Fracchiolla et al., 2016; Martínez-Mena et al., 2021a, 2021b; Morugán-Coronado et al., 2020; Ramos et al., 2010; Repullo-Ruibérriz de Torres et al., 2021; Vicente-Vicente et al., 2016). Almagro et al. (2016) observed in semiarid Mediterranean agroecosystems that rainfed almonds with reduced tillage and VC showed lower soil erosion rates and higher yields, soil organic carbon contents and aggregate stability than conventional treatments. Morugán-Coronado et al. (2020) suggested the use of permanent crops in the inter-row with minimum tillage and organic fertilization under Mediterranean climate conditions to improve soil quality properties, adaptation to drought and erosion events, without negative effects on the yield of tree crops. However, these authors highlighted the importance of the soil characteristics and climate conditions particular of each region on crop responses to SMP, especially in warm and dry environments. In this line, Ramos et al. (2010) proposed the use of VC in semiarid environments instead of frequently tilled management to increase the organic matter content in the soil improving its chemical, physical and biological activity. Nevertheless, these authors indicated that the higher water extraction by VC could negatively affect the almond orchard development and its yields. Therefore, possible competition for water and nutrients between woody crops and adjacent herbaceous species should be analyzed based on specific crop species, agricultural management practices and climate conditions (Morugán-Coronado et al., 2020).

In recent decades, time-series information obtained from remote sensing (RS)-based images has been broadly used for crop dynamics monitoring. Remote sensing has demonstrated its potential and effectiveness to carry out spatial-temporal monitoring of vegetation (Calera et al., 2017; Khaliq et al., 2019) through vegetation indices (VI) derived from remote sensing images. VI_s are sensitive to changes in vegetation in terms of physiological development, since they can reflect the growth and development adversities suffered by the crop by reducing the chlorophyll density or its biomass, which will cause a decrease in the VI value (Tucker, 1979; Tucker et al., 1981). This fact has favored its use as indicators of various biophysical parameters such as the vegetation fraction cover (canopy cover, CC), leaf area index, fraction of absorbed photosynthetically active radiation, crop coefficient (K_c), plant height, and chlorophyll and water content, among others (Alganci et al., 2014; Bausch and Neale, 1987; Pinter et al., 2003). The evolution of canopy biophysical parameters in woody crops has been characterized in different works through the normalized difference vegetation index (NDVI; Rouse et al., 1973) and Soil Adjusted Vegetation Index (SAVI; Huete, 1988) (Balbontín et al., 2017; Bellvert et al., 2018, 2021; Campos et al., 2010; Conesa et al., 2019; Zarate-Valdez et al., 2012). However, some authors call for caution in using VI_s due to their sensitivity of vegetation indices to canopy geometry (leaf angle distribution function, row orientation, and spacing), soil optical properties, sun position and the cloudiness (Baret and Guyot, 1991). Additionally, special attention need to be paid when trying to apply VI_s on heterogeneous canopies with a mixed combination of soils, weeds, cover crops and trees; since this kind of crops makes more difficult the discrimination and extraction of the VI of each single component (Xue and Su, 2017).

The temporal assessment of VI_s describes the time evolution of vegetation canopies and provides information regarding relative photosynthetic capacity (Asrar et al., 1984). NDVI and SAVI can be easily derived through satellites such as Sentinel-2 over large areas in near real time.

Another advantage of RS is that it allows obtaining information automatically on plant structures through the study or interpretation of images obtained from remote sensors. At the individual tree level, these images allow to acquire information on key parameters such as distance between trees, their location, and tree canopy diameter and volume, among others (Wagner et al., 2018). Nevertheless, the use of management practices such as VC may limit the usefulness of RS for characterizing woody crops (Aguirre-García et al., 2021; Burchard-Levine et al., 2021).

The main objective of this work was to evaluate the vegetative response of almond trees to sustained irrigation regime and soil management. The main hypothesis to be tested within the present study was whether VI_s derived from RS were a suitable methodology for almond water status and almond morphological parameters determination. This hypothesis was addressed by the comparison of NDVI and SAVI time-series with plant water status (stem water potential; Ψ_{stem}) and plant morphological measurement (trunk perimeter and canopy diameter) performed at ground level. Additionally, an automatic method to obtain CC through RGB aerial orthophotos was proposed.

2. Materials and methods

2.1. Experimental treatments and design

An experiment was performed in a 2.1 ha commercial young almond orchard (*Prunus dulcis* var. Belona) located in Hellín (38° 22' 53'' N, 1° 30' 32'' W; Albacete, Spain) (Fig. 1) during three agricultural campaigns (2018–2020). Almond trees were grafted on G-677 rootstock and planted in the spring of 2016 with a triangular planting with a spacing of 7 × 5 m. Currently, the trees have reached an average height of 2.5–3 m (Fig. S1).

The soil in the area is classified as Calciorthid having a loam soil texture, low content of organic matter (1.60 %) and a basic pH of 8.59. According to the Köppen-Geiger system, the climatology in the study area is classified as semi-arid steppe (Bsk). Average annual precipitation (P) and mean air temperature (T_{air}) for the period 1982–2012 were 307 mm and 17.2 °C, respectively (https://es.climate-data.org/). Specifically for the three considered seasons, the average T_{air}, relative humidity (RH) and solar radiation (R_s) were 17.5 °C, 64 % and 18.4 MJ m^{-2} d^{-1}; whereas the annual reference evapotranspiration (ET_o) and P were 1255 and 310 mm, respectively (Fig. 2).

Pruning, fertilization and pest, disease and weed control were carried out by the farm owner. In brief, pruning was moderate and performed manually in winter. The amount of macronutrients applied in the forms of N, P_2O_5 and K_2O, were 25, 15 and 20 kg ha^{-1} in 2018; 35, 20 and 30 kg ha^{-1} in 2019; and 50, 30 and 50 kg ha^{-1} in 2020, respectively. A winter treatment was given every year for insect and disease control, and only in 2020 trees were treated for the almond seed wasp control. Weeds in the almond row were avoided by treating with herbicides during spring and autumn.

The experimental design consists of 5 treatments (Table 1) stablished for analyzing the effects of various agricultural management factors in an almond orchard including sustained irrigation regime and soil management on some physiological and morphological parameters. Fig. 3 summarizes the flowchart followed in the present study. The 5 treatments were randomly replicated in a design of 3 complete randomized blocks. Each experimental unit, treatment replicate, occupied 700 m^2

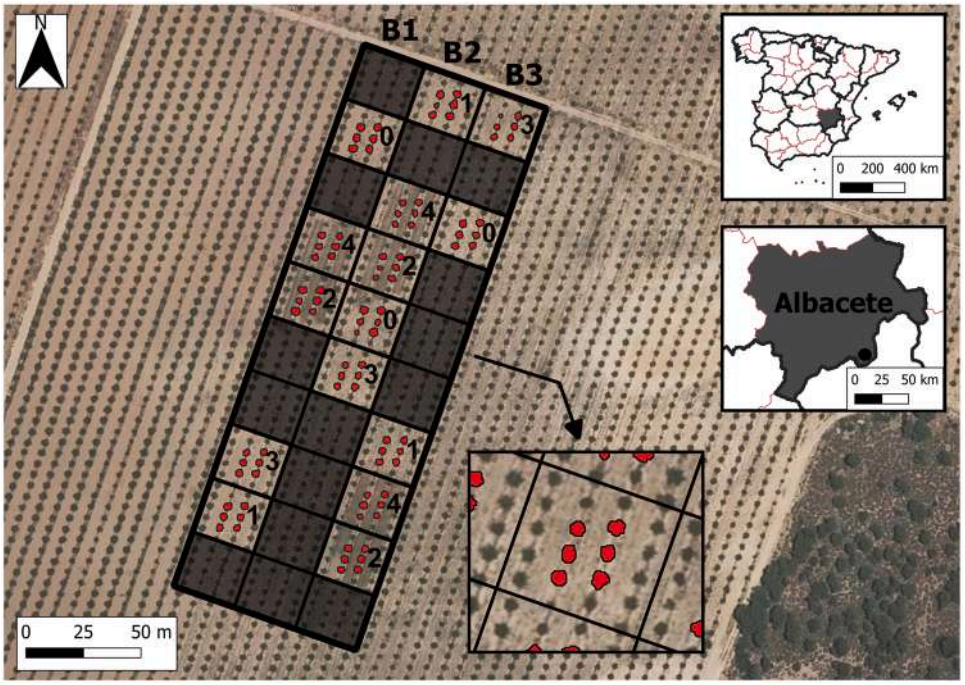

Fig. 1. Map of the study area located in southern Spain in Hellín (Albacete) (38° 22' 53'' N, 1° 30' 32'' W). Treatments (ID 0–4, see Table 1) per block (B1-B3) are also shown. An example of control trees is shown in greater detail. Grey areas correspond with additional treatments not considered in the present study.

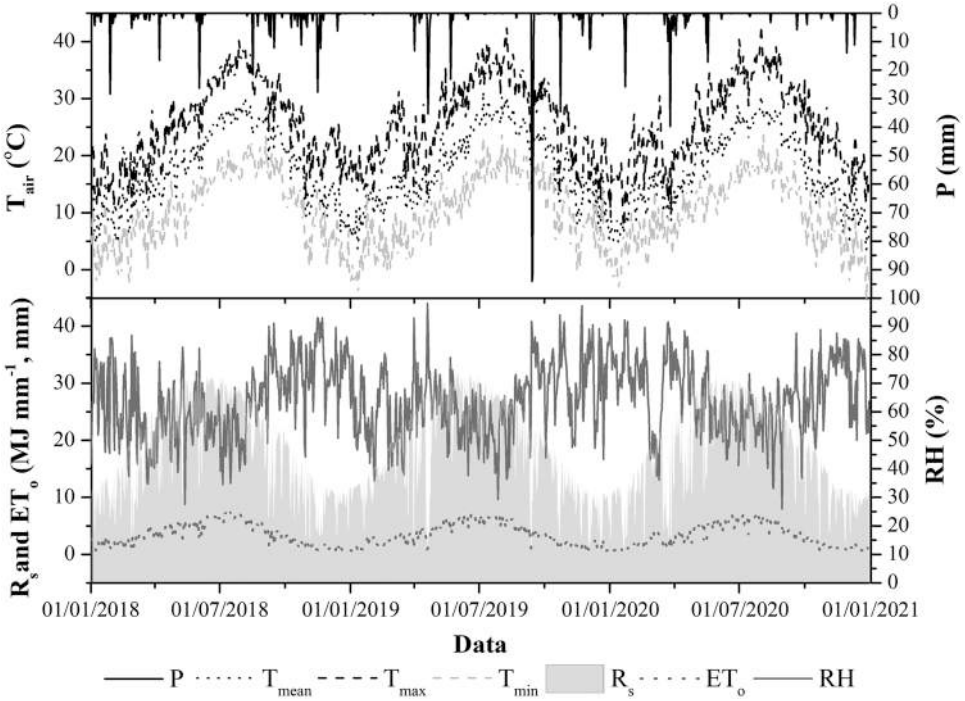

Fig. 2. Daily maximum, minimum and mean air temperature (T_{max}, T_{min} and T_{mean}), precipitation (P), solar radiation (R_s), reference evapotranspiration (ET_o) and relative humidity (RH) recorded from Cieza meteorological station, for the period 2018–2020.

approximately, containing 20 trees in most cases. The six central trees of each experimental unit have been used as "experimental trees" for the physiological and morphological determinations whereas the rest served as guard trees (Fig. 1).

The effect of sustained irrigation regime (in terms of percentage of ET_c satisfied during the irrigation season) was analyzed by comparing a control treatment where irrigation satisfied maximum crop water requirements (≈ 100 % of crop evapotranspiration, ET_c) with two SDI strategies that introduced moderate or severe water restrictions throughout the season (67 % and 33 % of ET_c, respectively) (Table 1). The drippers spacing within the line was 0.75 m with a dripper flow rate of 1, 2 or 3 L h^{-1}, in the severe, moderate and non-water restrictions treatments, respectively. Net water requirements were estimated weekly by subtracting effective P to ET_c, the latter calculated as the product of ET_o and K_c. Daily ET_o was obtained from the nearest (less than 10 km from the experimental site) meteorological station located in Cieza (38°

Table 1
Main characteristics of the different treatments and Irrigation volumes (mm) of the treatments analysed for the 2018–2020 irrigation seasons. ID: identifier. SDI: sustained deficit irrigation. SDI_M: moderate sustained deficit irrigation. SDI_S: severe sustained deficit irrigation. ET_c: crop evapotranspiration. BS: bare soil. VC: vegetation cover.

ID	Treatment	Irrigation strategy (%ET_c)	Soil management	Irrigation volume (mm)		
				2018	2019	2020
0	Control	100 %	BS	186	206	486
1	SDI_M-BS	67 %	BS	125	138	326
2	SDI_M -VC	67 %	VC			
3	SDI_S-BS	33 %	BS	61	68	160
4	SDI_S -VC	33 %	VC			

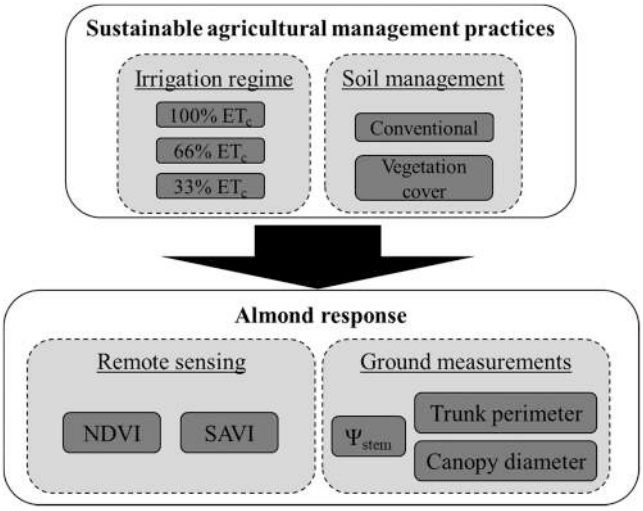

Fig. 3. Flowchart of the methodology followed in the present study.

17' 24'' N, 1° 29' 56'' W; Murcia) belonging to the Sistema de Información Agroclimática para el Regadío (SIAR, http://eportal.mapa.gob.es/websiar/Inicio.aspx) agrometeorological station network. Regarding the K_c, the values used were those proposed by Espadafor et al. (2015) and corrected with the percentage of the shaded area of the control trees that takes into account the average shaded area of the tree (m^2) and the planting frame (m^2) (Fereres et al., 1982).

For evaluating the effect of soil management, two soil management practices were compared: (i) conventional soil management, and (ii) use of VC (Table 1). In the conventional soil management, the soil was kept bare (BS, bare soil) by herbicide applications in the rows and spring and autumn tillage between the rows. Alternatively, the use of VC consisted of sowing in the inter-rows a mixed cover of legumes (15 % *Onobrychis viciifolia,* 15 % *Vicia sativa* and 10 % *Trifolium alexandrinum*) and gramineous (20 % *Festuca arundinacea,* 20 % *Dactylis glomerata* and 20 % *Lolium rigidum*). Specifically, VC was sown in January 2018 and December 2019 and re-sprouted during 2020.

Different water meters were installed to monitor irrigation applications. Table 1 shows the irrigation volumes applied to the different treatments during the three irrigation seasons.

2.2. Remote sensing imagery

Sentinel-2A and 2B satellites imagery were used for evaluating the effect of the considered management factors. These freely-available images, downloaded from Copernicus Open Access Hub (https://scihub.copernicus.eu/dhus/#/home), corresponded with orthorectified Bottom-Of-Atmosphere reflectances (level-2A product). The spatial resolution of Sentinel-2 imagery ranges from 10 to 60 m depending on the considered spectral band. In this study, only 10 m spatial resolution bands were used (see section "2.2.1. Vegetation Indices"). Satellite revisit frequency in the study site is 5 days when considering both Sentinel-2A and 2B satellites together. For the considered period (2018–2020), a total of 200 satellite images were available. However, for the purpose of this study, it worsened by the presence of clouds on the study site (≈ 65 % for the 2018–2020 period), resulting in a total of 70 cloudless available satellite images (Table 2).

2.2.1. Vegetation indices

For each treatment and year analyzed, the vegetation temporal evolution was examined through the NDVI and SAVI derived from Sentinel images. The NDVI is defined as the normalized difference of the near infrared (ρ_{NIR}) and red (ρ_{RED}) reflectances:

$$NDVI = \frac{\rho_{NIR} - \rho_{RED}}{\rho_{NIR} + \rho_{RED}} \quad (1)$$

where ρ_{NIR} and ρ_{RED} correspond to band 8 (0.833 μm) and band 4 (0.665 μm) of the Sentinel satellite images, respectively. NDVI values range from -1 to $+1$. Dense vegetation presents positive and high NDVI values, bare soil has near to zero values, and clouds, snow and water have negative values.

Similarly, SAVI is computed from ρ_{NIR} and ρ_{RED}, but its calculation includes L coefficient (assumed in this study equal to 0.5) in order to correct the influence of soil brightness in areas where vegetative cover is low (Huete, 1988):

$$SAVI = \frac{\rho_{NIR} - \rho_{RED}}{\rho_{NIR} + \rho_{RED} + L} * (1 + L) \quad (2)$$

2.2.2. Geometric correction of Sentinel-2 images

Sentinel-2A and 2B images show a small geometric displacement

Table 2
Acquisition dates of the images used in the study (S2A: Sentinel-2A; S2B: Sentinel-2B).

2018		2019		2020	
01 January 2018	S2A	06 January 2019	S2A	06 January 2020	S2B
21 January 2018	S2A	26 January 2019	S2A	11 January 2020	S2A
15 February 2018	S2B	05 February 2019	S2A	16 January 2020	S2B
22 March 2018	S2A	25 February 2019	S2A	10 February 2020	S2A
27 March 2018	S2B	17 March 2019	S2A	15 February 2020	S2B
16 May 2018	S2B	27 March 2019	S2A	11 March 2020	S2A
15 June 2018	S2B	11 April 2019	S2B	26 March 2020	S2B
20 June 2018	S2A	16 April 2019	S2A	20 May 2020	S2A
30 June 2018	S2A	26 April 2019	S2A	30 May 2020	S2A
10 July 2018	S2A	16 May 2019	S2A	14 June 2020	S2B
30 July 2018	S2A	31 May 2019	S2B	29 June 2020	S2A
04 August 2018	S2B	10 June 2019	S2B	04 July 2020	S2B
09 August 2018	S2A	15 June 2019	S2A	19 July 2020	S2A
29 August 2018	S2A	25 June 2019	S2A	24 July 2020	S2B
23 September 2018	S2B	15 July 2019	S2A	29 July 2020	S2A
03 October 2018	S2B	25 July 2019	S2A	08 August 2020	S2A
13 October 2018	S2B	04 August 2019	S2A	13 August 2020	S2B
07 December 2018	S2A	14 August 2019	S2A	28 August 2020	S2A
17 December 2018	S2A	24 August 2019	S2A	12 September 2020	S2B
		03 September 2019	S2A	27 September 2020	S2A
		18 September 2019	S2B	07 October 2020	S2A
		03 October 2019	S2A	17 October 2020	S2A
		13 October 2019	S2A	27 October 2020	S2A
		12 November 2019	S2A	01 November 2020	S2B
		22 December 2019	S2A	01 December 2020	S2B
				26 December 2020	S2A

from one to another date (Fig. 4). If not corrected, it could lead to unreal results, especially when dealing with small experimental units as happens in the present study. The methodology followed to correct such displacements consisted on generating a vector file taking an Orthophoto of the Spanish National Plan for Aerial Orthophotography (PNOA 2019; https://pnoa.ign.es/) as reference. This vector file contains (i) two dirt roads located on the west and on the north of the study plot; and (ii) the experimental units. This methodology assumes that the distance from these roads to each one of the experimental plots was invariant and well known. Thus, the vector file generated on PNOA orthophoto was displaced for each satellite date taken as reference the dirt roads in each one of the Sentinel images. In this way, shifting the vector file instead of georeferencing the raster satellite images will preserve the original pixel values avoiding signal modifications caused by the georeferencing of the image (e.g. using a cubic convolution resampling). This pre-procedure was performed using ArcGIS (v10.2; Esri, Redlands, CA, USA). Fig. 4 shows an example comparing the analyzed plot from a PNOA orthophoto and from two Sentinel images (20 May 2020 and 1 November 2020). Displacement between Sentinel images can be easily observed from adjacent trails to the plot.

2.3. Canopy cover from PNOA orthophotos

Canopy area of each control tree (Fig. 1) was calculated using PNOA RGB orthophotos of October 2018 and June 2019. Such orthophotos have a 25 cm pixel size that allowed distinguishing between tree and soil surfaces within the analyzed experimental plots. The segmentation was carried out using the open-source Semi-Automatic Classification Plugin (Congedo, 2021), developed for QGIS software (https://www.qgis.org/es/site/) (version QGIS 3.12 'Bucureşti' provided by QGIS Development Team). Representative areas of almond trees and areas of BS were manually selected for obtaining the typical spectral signature of the vegetation and the soil, which represents the basis for their automatic discrimination. Finally, the obtained segmentation was visually checked for correcting any possible error in the classes assignment.

The CC (%) values obtained through PNOA orthophotos were linearly correlated with the CC measured in field (see section "2.4.2. Trunk perimeter and canopy diameter") in two dates close to those of the PNOA acquisition date (Fig. S2). Concretely, the dates of the measurements field were 11 November 2018 and 5 July 2019.

2.4. Field determinations

Physiological and morphological determinations of Ψ_{stem}, trunk perimeter and canopy diameter were performed at different dates during the three years analysed (Fig. 5).

2.4.1. Stem water potential

Measurements of Ψ_{stem} (MPa) were performed once or twice a month

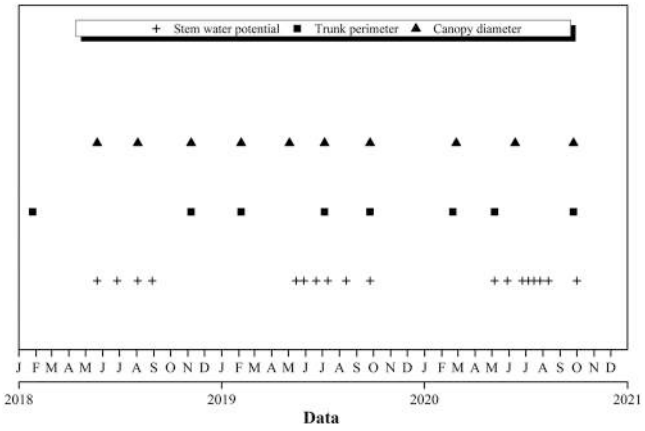

Fig. 5. Dates of field determinations during the period 2018–2020.

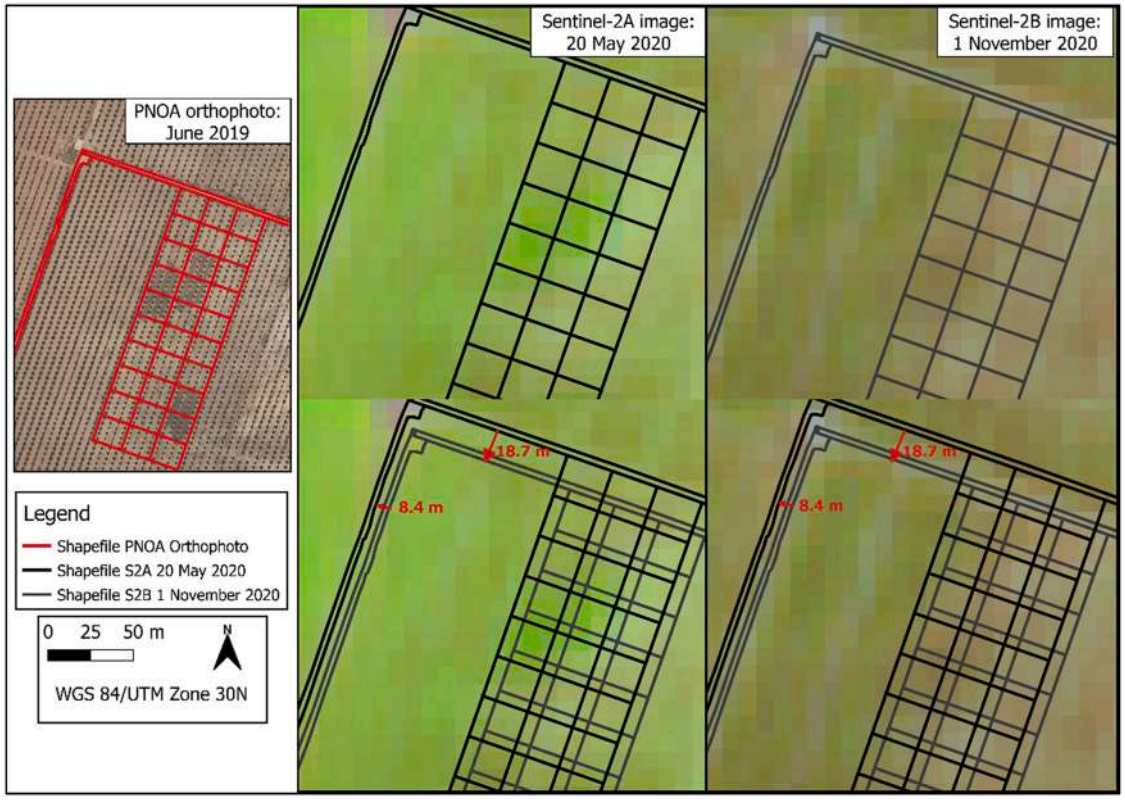

Fig. 4. Example of geometric displacement between Sentinel images (20 May 2020 and 1 November 2020).

(Fig. 5) by means of a Scholander-type pressure chamber (Model 600, PMS Instrument Company, Albany, OR, USA). Two (in 2018) or three (in 2019 and 2020) mature leaves from two different trees were selected for each experimental unit. The leaves were enclosed in plastic bags covered with aluminium foil at least 1 h before performing the measurements, which were conducted between 12:00 and 14:00 h solar time. Ψ_{stem} measurements were performed in all treatments except for the first irrigation season where no measurements were made in SDI_M-VC.

2.4.2. Trunk perimeter and canopy diameter

Trunk perimeter was measured manually with a tape measure prior to the bifurcation of the branches with respect to the trunk at a distance of about 0.4 m above the ground. The measurements were performed twice, during 2018, or three times, during 2019 and 2020 (Fig. 5).

Canopy diameter was measured with a marked pole with a band spacing of 10 cm three times during 2018 and 2020 and four times during 2019 (Fig. 5). From these diameters, CC (%) was estimated as the area occupied by the three (assumed as a circle of mean diameter) divided by the planting framework (7 x 5 m).

Trunk perimeter was measured in two trees for each experimental unit (6 trees per treatment) and canopy diameter was measured in four trees for each experimental unit (12 trees per treatment).

The trunk perimeter and the CC were linearly interpolated between the field measurement dates and correlated with the NDVI and SAVI values on a selected date for every year chosen during the second half of May (16 May 2018, 16 May 2019 and 20 May 2020). This date coincided when the growth of the almond trees was maximum and when great differences in the values of NDVI and SAVI were observed between treatments with and without VC, before the summer, avoiding a possible summer vegetative stop caused by high temperatures. The analysis was performed distinguish between treatments with VC, SDI_M-VC and SDI_S-VC, and treatments with a conventional soil management, SDI_M-BS and SDI_S-BS. All CC measurements performed were also correlated with the NDVI and SAVI. Thus, the VI_s values were linearly interpolated between adjacent dates to obtain the daily values for every treatment analyzed along the study.

2.5. Statistical analysis

In the analyses of effects studied (sustained irrigation regime and soil management), the differences found between treatments were analyzed through the temporal evolution of NDVI, SAVI, Ψ_{stem}, trunk perimeter and canopy diameter by means of randomized complete block of analysis of variance (ANOVA). Statistix 9 (Analytical Software, Tallahassee, USA) was the software used. Significant differences between means were assessed with an honest significant difference (HSD) Tukey test ($p \leq 0.05$).

Relationships between the morphological determinations of trunk perimeter and CC versus the temporal evolution of NDVI and SAVI for the different treatments were performed and analyzed through the root mean square error (RMSE) and the coefficient of determination (R^2). Only the pixels completely included within each experimental unit were analyzed for each image utilized.

3. Results

3.1. Temporal trend of NDVI, SAVI and plant water status

In general, all treatments showed a similar trend in the temporal evolution of NDVI, SAVI and Ψ_{stem} (Figs. 6–8). Specifically, for the considered period, mean irrigation season NDVI of the entire study area increased progressively from 0.22 in 2018 to 0.31 in 2019 and 0.36 in 2020. In a similar way, mean irrigation season SAVI of the entire study area increased progressively from 0.17 in 2018 to 0.25 in 2019 and 0.26 in 2020. Regarding the Ψ_{stem}, a decreasing trend in all treatments was observed during the summer months for all irrigation seasons considered, with values of about −1.0 to −1.5 MPa at the beginning of the irrigation season, reaching the most negative values at the end of July-

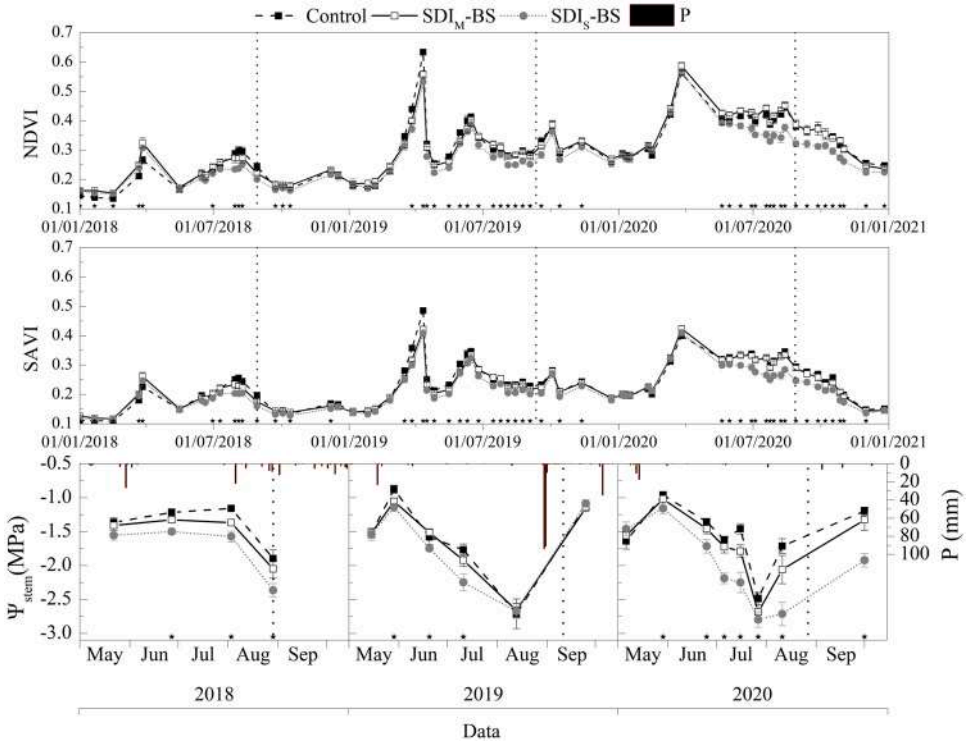

Fig. 6. Temporal evolution of the NDVI, SAVI and the stem water potential (Ψ_{stem}) for the control, SDI_M-BS and SDI_S-BS treatments. Error bars represent the standard error. Black asterisks indicate statistically significant differences between treatments at $p \leq 0.05$. Precipitation (P) is also shown. Dotted lines indicate harvest dates. For a detailed description of the treatments, the reader is referred to Table 1.

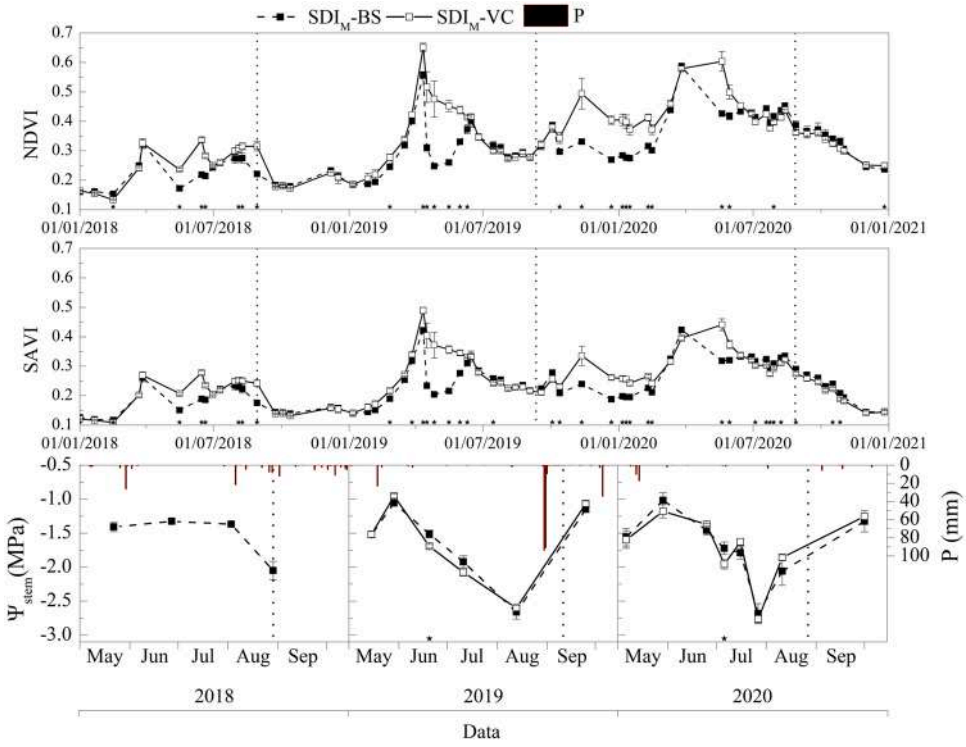

Fig. 7. Temporal evolution of the NDVI, SAVI and the stem water potential (Ψ_{stem}) for the SDI$_M$-BS and SDI$_M$-VC treatments. Error bars represent the standard error. Black asterisks indicate statistically significant differences between treatments at $p \leq 0.05$. Precipitation (P) is also shown. Dotted lines indicate harvest dates. For a detailed description of the treatments, the reader is referred to Table 1.

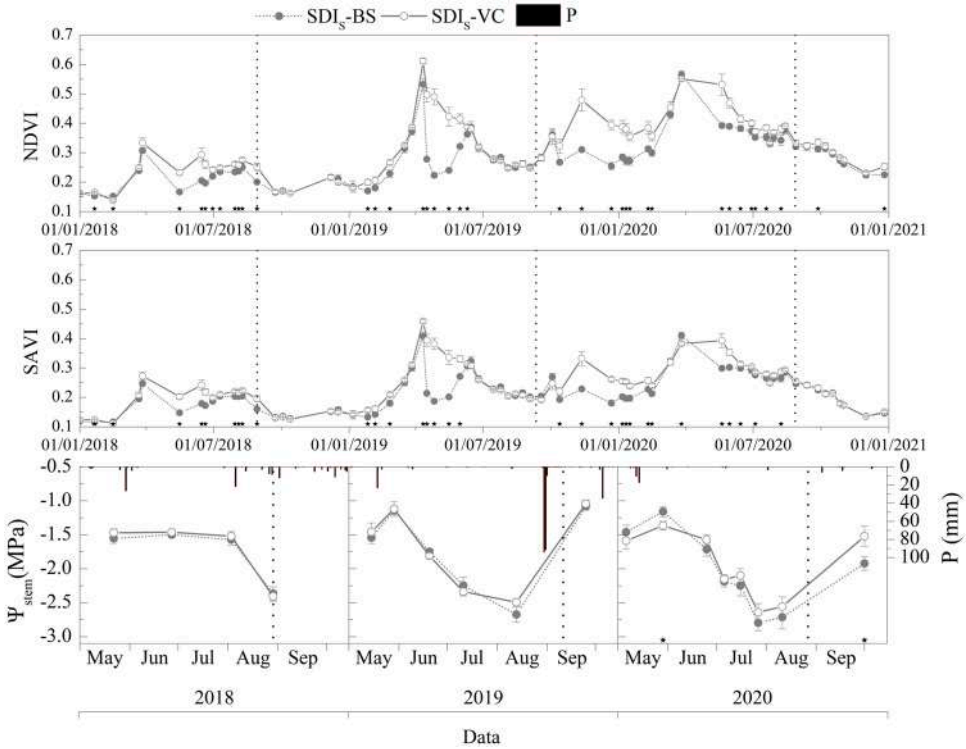

Fig. 8. Temporal evolution of the NDVI, SAVI and the stem water potential (Ψ_{stem}) for the SDI$_S$-BS and SDI$_S$-VC treatments. Error bars represent the standard error. Black asterisks indicate statistically significant differences between treatments at $p \leq 0.05$. Precipitation (P) is also shown. Dotted lines indicate harvest dates. For a detailed description of the treatments, the reader is referred to Table 1.

August (−2.5 to −3.0 MPa; Figs. 6–8). Additional information about statistical analysis is shown in Tables S1-S4.

3.1.1. Effects of sustained irrigation regime

When analyzing the effect that sustained irrigation regime had on almond NDVI and SAVI (Fig. 6), it was observed that control and SDI_M-BS treatments generally presented significantly higher NDVI and SAVI values than SDI_S-BS treatment. The occurrence of these differences varied from year to year, emerging at late July in 2018, late March and late June in 2019 (for the differences between control versus SDI_S; and SDI_M versus SDIs, respectively); and at mid-May in 2020 (Fig. 6). On the contrary, no significant differences were observed between control and SDI_M-BS treatments, except for the three initial months of the experiment and 4th August 2018 (Table S1); and 27th March (only for SAVI), 11th April, 31st May, 4th August (only for SAVI) and 3rd September 2019 (Table S2); where the control presented significantly higher NDVI and SAVI values (Fig. 6).

The same discrepancies among treatments were also observed in terms of Ψ_{stem}, with the control and SDI_M-BS treatments generally not showing statistical differences among them, but having less negative Ψ_{stem} values than SDI_S-BS treatment (Fig. 6). Specifically, the latter presented significantly more negative Ψ_{stem} by 23 % and 14 %, when compared to the control and SDI_M-BS treatments, respectively (Table S4).

3.1.2. Effects of soil management

The presence of VC resulted in a significant increase of the NDVI and SAVI when compared to BS treatments under both SDI_M and SDI_S irrigation strategies (Figs. 7 and 8). Specifically, in 2018 these differences in NDVI and SAVI appeared from May to August (except in July), with a mean NDVI increase of 34 % and 19 % for SDI_M and SDI_S, respectively; and a mean SAVI increase of 28 % and 22 % for SDI_M and SDI_S, respectively. In 2019, the effect of the ground cover resulted significant between early April and early June, causing an average NDVI and SAVI increase of 50–52 % (Table S2); and also from mid-October of 2019 to mid-February of 2020, with a mean NDVI and SAVI increase of 36 % and 25 % respectively (Tables S2 and S3). Additionally, statistical differences between BS and VC treatments in terms of NDVI and SAVI, concentrated during May of 2020 with an average NDVI and SAVI increase of 28–29 % and 23–27 %, respectively (Figs. 7 and 8).

Such differences in terms of NDVI and SAVI did not translate into significant differences of Ψ_{stem}, neither under SDI_M nor SDI_S (except for 20th June 2019 and 6th July 2020 for SDI_M and 29th May and 1st October 2020 for SDI_S; Figs. 6 and 7).

3.2. Temporal trend of trunk perimeter and canopy diameter

The temporal evolution of the trunk perimeter and the canopy diameter for every treatment and effect analyzed showed a similar pattern during the three years examined (Fig. 9). Both parameters increased progressively after the winter period until the following winter period throughout the three years of study. The mean initial trunk perimeter for the entire study site was 7.5 cm, reaching values of 26–32 cm at the end of 2020. Average canopy diameter for the study site also increased progressively from 1.3 m at the beginning of 2018 to 3.5 m at the end of 2020. Additional information about statistical analysis is shown in Tables S5 and S6.

Regarding the effect of the sustained irrigation regime on trunk perimeter, SDI_S-BS treatment resulted in significant reductions of trunk perimeter (≈ 15–13 %) in comparison to the control and SDI_M-BS treatments in most evaluated dates (Fig. 9a). The presence of VC (SDI_M and SDI_S) resulted in an 8–7 % lower trunk perimeter at the end of 2020 irrigation season when compared to BS treatments (Fig. 9c and e).

Sustained irrigation regime also showed a significant effect on canopy diameter. Specifically, SDI_S-BS treatment resulted in significant lower canopy diameters than control in the last two measurement dates (mean canopy diameters reduction of 0.45 m) (Fig. 9b and Table S6). Significant canopy diameter reductions of about 0.37 m were discontinuously observed throughout the study period between SDI_S-BS and SDI_M-BS treatments, although these treatments showed no differences at the end of the experiment. The presence of VC also caused a reduction of canopy diameter of 0.34–0.37 m when compared to BS both under SDI_M and SDI_S irrigation regimes from November 2018 (SDI_M) and July 2019 (SDI_S) to the end of 2020 (Fig. 9d and f).

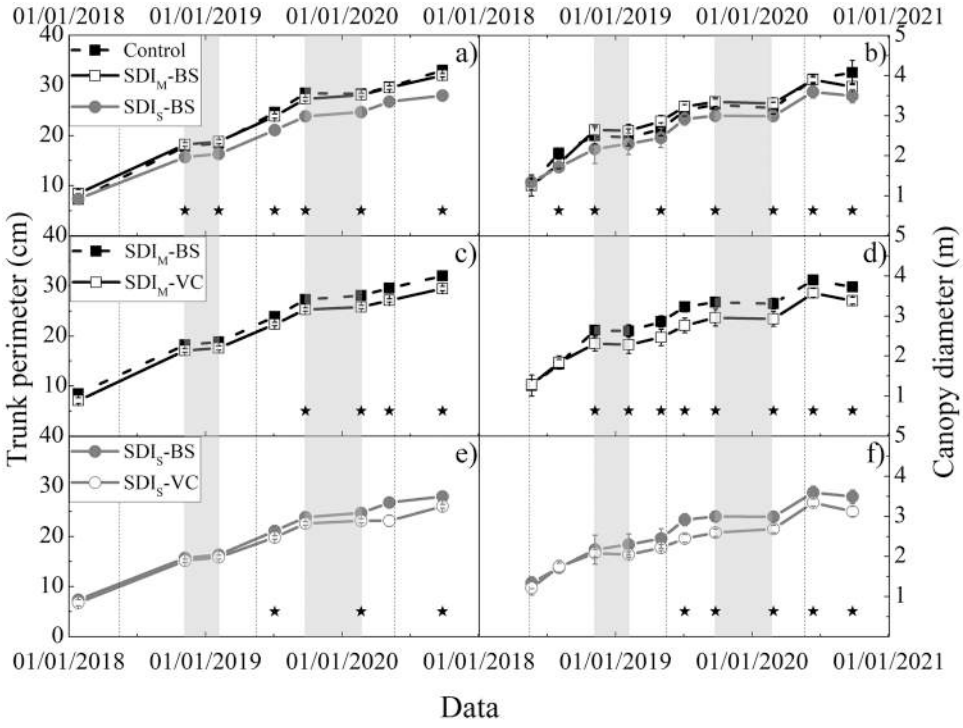

Fig. 9. Temporal evolution of the trunk perimeter and canopy diameter comparing the treatments according to (a and b) irrigation regime; and (c - f) soil management. Error bars represent the standard error. The black asterisks indicate statistically significant differences between treatments at $p \leq 0.05$. Greys boxes indicate the winter rest periods. Dashed lines indicate the selected dates used to correlate trunk perimeter and canopy diameter with the NDVI and SAVI values (Figs. 10–11). For a detailed description of the treatments, the reader is referred to Table 1.

3.3. Relationships between remote sensing measurements and morphological determinations

3.3.1. Vegetation Indexes-Trunk perimeter

Trunk perimeter and VI_s showed a high correlation both for BS and VC treatments, with R^2 values of 0.94–0.95 and RMSE values ranging from 1.49 to 1.86 cm (Fig. 10a, c). However, this relationship varied depending on the soil management and the differences between BS and VC were more evident as the tree was bigger (i.e., higher trunk perimeter). For instance, trees with a similar trunk perimeter of 10 cm exhibited mean NDVI differences of about 0.10 between BS and VC treatments (NDVI of 0.16 and 0.26 for BS and VC, respectively); whereas these NDVI differences reached values of 0.20 for trunk perimeters close to 25 cm (NDVI of 0.36 and 0.56 for BS and VC, respectively) (Fig. 10a). However, these differences between BC and VC treatments in terms of SAVI resulted lower than for NDVI, being 0.07 (SAVI of 0.14 and 0.21 for BS and VC, respectively) and 0.17 (SAVI of 0.26 and 0.43 for BS and VC, respectively) for trunks perimeters of 10 and 25 cm, respectively (Fig. 10c).

3.3.2. Vegetation Indexes-Canopy cover

When correlating VI_s and CC observed at the seasonal moment of maximum almond growth (Fig. 10b, d), close relationships were obtained both for BS and VC treatments (R^2 from 0.80 to 0.91). Additionally, the dispersion of the relationship obtained for both VI_s was higher for VC treatments than for BS, with RMSE values of 4.05–4.07 % and 3.36–3.45 %, respectively.

As observed also for trunk perimeter, the obtained relationship varied depending on the soil management and being the differences between VC and BS more evident as the tree CC was higher. Thus, trees with a similar CC of 5 % exhibited mean NDVI differences of about 0.10 between BS and VC treatments (NDVI of 0.16 and 0.26 for BS and VC, respectively); whereas these NDVI differences reached values of 0.25 for CC close to 25 % (NDVI of 0.35 and 0.60 for BS and VC, respectively) (Fig. 10b). As for the relationship obtained for the trunk perimeter, these differences between BC and VC treatments in terms of SAVI resulted lower than for NDVI, being 0.07 (SAVI of 0.15 and 0.22 for BS and VC, respectively) and 0.18 (SAVI of 0.27 and 0.45 for BS and VC, respectively) for canopy covers of 5 % and 2 %, respectively (Fig. 10d).

On the other hand, when considering all canopy measurements performed during the entire almond growth and development cycle (Fig. 11a, b), the strength of the relationships diminished, with R^2 values of NDVI relationships of 0.60 and 0.24 for BS and VC, respectively; and R^2 values of SAVI relationships of 0.47 and 0.14 for BS and VC, respectively. Accordingly, the dispersion observed considerably increased for BS and VC, with RMSE of 6.27 % and 6.53 % for NDVI,

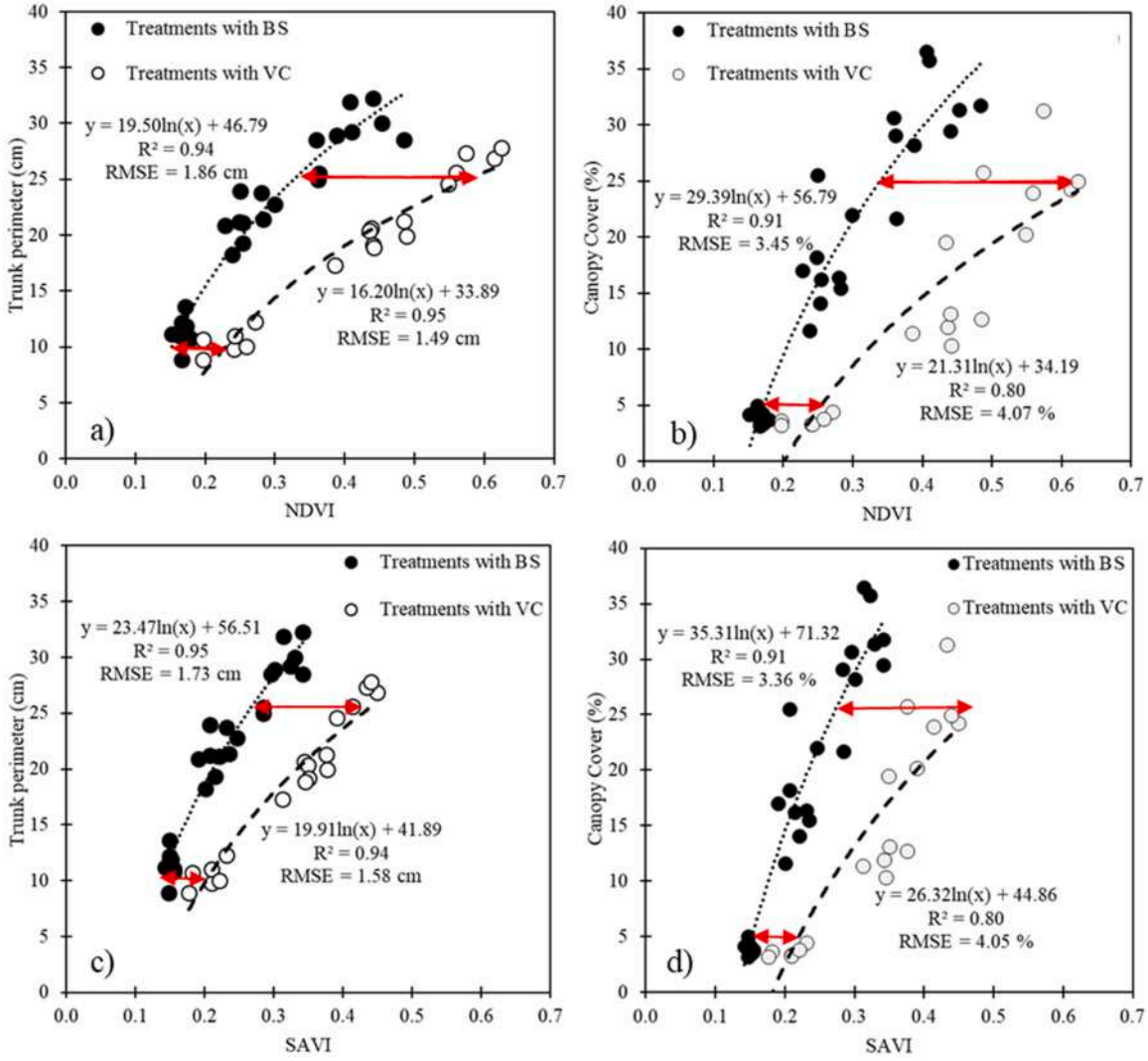

Fig. 10. Relationships between (a-b) NDVI and (c-d) SAVI with trunk perimeter, and canopy cover for vegetation cover (VC) (SDI_M-VC and SDI_S-VC) and bare soil treatments (BS) (Control, SDI_M-BS and SDI_S-BS) at the maximum season almond growth moment. Red arrows represent VI_s differences between VC and BS treatments, for two specific (a) trunk perimeters (i.e., 10 and 25 cm), and (b) canopy covers (i.e., 5 % and 25 %).

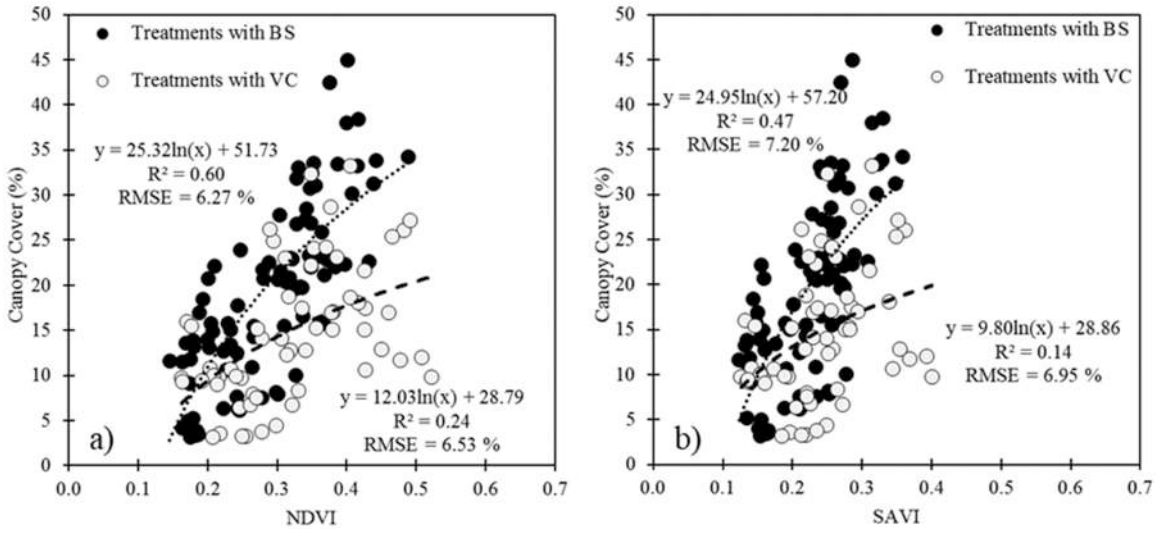

Fig. 11. Relationship between (a) NDVI and (b) SAVI; with canopy cover for vegetation cover (VC) (SDI_M-VC and SDI_S-VC) and bare soil treatments (BS) (Control, SDI_M-BS and SDI_S-BS) for all field measurement dates of canopy cover.

respectively; and 7.20 % and 6.95 % for SAVI, respectively.

4. Discussion

Almond tree response to different management practices has been widely analyzed using different physiological and morphological determinations capable of estimating plant water status and vegetative growth, among other parameters (Bellvert et al., 2021; Egea et al., 2013). Sustained irrigation regime and soil management presented clear differences in VI_s values, tree dimensions and Ψ_{stem} among their respective treatments (Figs. 5–11 and 14). Specifically, the application of SDI_S (i.e., 33 % of ET_c) resulted in lower VI_s values and vegetative growth (i.e., trunk perimeter and canopy diameter) and in higher water stress (i.e., more negative Ψ_{stem} values) when compared to the control treatment. However, the application of SDI_M (i.e., 67 %) did not negatively affect the almond orchard in terms of VI_s, Ψ_{stem}, trunk perimeter and canopy diameter, since in general they did not differ from what observed in the control treatment (Tables S1-S6). In a 6-year long experiment in southern Spain with mature almond trees, Moldero et al. (2021) found greater differences in Ψ_{stem} and CC between SDI_M (i.e., 65 % of ET_c) and control treatments. Likewise, Egea et al. (2013), obtained significant differences in Ψ_{stem} and trunk perimeter between a mild-to-moderate SDI (irrigated at 75 % of ET_c during 2001–2003 and at 60 % of ET_c during 2004–2006), a moderate-to-severe SDI (irrigated at 60 % of ET_c during 2001–2003 and at 30 % of ET_c during 2004–2006) and control treatments in an almond orchard also in southeast Spain. Such discrepancies in comparison to our experiment could be explained by the longer water stress time exposure (i.e. experiment duration) and the more mature trees used by Moldero et al. (2021) and Egea et al. (2013).

The presence of VC in the inter-row increased the pixels VI_s while almond trees maintained the same water status under BS and VC treatments (see Ψ_{stem} in Figs. 6 and 7). Nevertheless, this higher canopy vigor of BS trees in 2020 was not well captured by the VI_s, which showed no differences between BS and VC. It highlights one of the main limitations of Sentinel-2 satellite for assessing heterogeneous crops. The 10 m spatial resolution of Sentinel-2 satellite images did not allow differentiating between the almond canopy, the BS and the VC in the inter-row, resulting in a heterogeneous pixel containing a mixture of the signals of the different surfaces. In this sense, the use of high resolution images as those acquired by drones or aircraft could help to better characterize the agricultural system and thus the partitioning of latent heat flux (and therefore, ET_c) between the almond, the BS and the VC. However, further studies are required for a better understanding of the long-term effects that VC could generate on soil physical, biological and chemical properties, including soil erosion processes, soil fertility, carbon stocks and other agricultural ecosystem services (De Leijster et al., 2020; Martínez-Mena et al., 2021a, 2021b; Ramos et al., 2010). Even if numerous works have been carried out in rainfed almond on this subject, additional studies are especially necessary in irrigated almond orchards where there are few bibliographic works on the matter.

As in other previous works carried out in woody crops (Conesa et al., 2019; Zarco-Tejada et al., 2012) the relationship between VI_s (NDVI and SAVI) and Ψ_{stem} has shown a low positive correlation between the different treatments (results not shown). These findings highlight the limitation of VI such as NDVI or SAVI for identifying short terms variations of plant water status, other than the stress reflected as a reduction or lesser expansion of VC. Alternatively, the strong relationship between canopy transpiration and surface temperature (González-Dugo et al., 2020) has allowed the use of other thermal indices such as the Crop Water Stress Index (CWSI) which have shown a better relationship with the Ψ_{stem} (Bellvert et al., 2018; Conesa et al., 2019; García-Tejero et al., 2017; González-Dugo et al., 2020).

On the contrary, NDVI and SAVI were able to capture structural differences of the vegetation in terms of trunk perimeter and CC, both with presence of VC in the inter-row and under conventional soil management. Specifically, the relationships between trunk perimeter and CC versus the VI_s showed strong logarithmic correlations both for BS and VC treatments. However, CC-VI_s relationships presented higher dispersions than trunk perimeter-VI_s, probably due to the artificial influence that the pruning operations had on the canopy size (but not in trunk perimeter). The presence of VC had a clear influence of the obtained relationships showing a NDVI displacement of about 0.10–0.25; and a SAVI displacement of about 0.07–0.18; for trunk perimeter and CC (Fig. 10) depending of the tree size and VC development. The reason of these lower differences between BS and VC in terms of SAVI when compared to NDVI could be due to the fact that SAVI, in its formulation, already applies a correction for the influence of soil brightness, especially in areas where vegetative cover is low (Huete, 1988). Even so, obtaining two different relationships (one for VC and other for BS) instead of using a unique one considering VC and BS together, will allow a better characterization of the morphological parameters from VI_s, reducing the dispersion and associated errors of such determinations. Additionally, the relationship between CC and VI_s improved when considering the moment of maximum almond growth (second half of May for every year), coinciding also with the greatest differences in the values of NDVI

and SAVI between BS and VC treatments (Fig. 10b, d). In this way, the dispersion caused by differences in VC development along the irrigation season was reduced (Fig. 10b, d and 11).

VI have been used to estimate crop coefficients using RS images for individual and mixed crops, as well as in natural ecosystems (Bausch and Neale, 1987; Campos et al., 2010; Choudhury et al., 1994; Duchemin et al., 2006; Er-Raki et al., 2007; Glenn et al., 2011; González-Dugo and Mateos, 2008; Hunsaker et al., 2003, 2005; Mateos et al., 2013; Pôças et al., 2015). Since the water requirements of woody crops vary depending on tree size and the shaded area percent (Fereres et al., 1982), tree growth measures such as CC can be used to adjust the necessary crop coefficients to estimate ET_c by improving the standard and tabulated estimates of water requirement (Trout et al., 2008). In this sense, numerous works have determined tree canopy geometric characteristics in woody crops and forest trees through high resolution satellite images such as QuickBird (Ozdemir, 2008; Whiteside and Ahmad, 2008), WordView-2 (Chemura et al., 2015; Verma et al., 2016; Wagner et al., 2018) or WordView-3 (Johansen et al., 2020; Rahman et al., 2018). Another works have employed airborne or UAV images (Bellvert et al., 2021; Díaz-Varela et al., 2015; Jiménez-Brenes et al., 2017; Johansen et al., 2020; Sarron et al., 2018) and LIDAR (Arenas-Corraliza et al., 2020; Borlaf-Mena et al., 2019; Popescu et al., 2003; Underwood et al., 2016; Verma et al., 2016; Wang et al., 2021). In this work, the close to 1:1 linear correlation obtained between the CC determined from PNOA orthophotos and that obtained from field measurements (Fig. S2), demonstrated the potential and accuracy of using high spatial resolution imagery (as the PNOA orthophotos) for deriving CC. This methodology presents important advantages compared to field measurements. Manual field measurements should be carried out periodically to represent variations in trees growth and therefore it is a time-consuming task (Wagner et al., 2018). Additionally, field measurements are not able to capture the irregular shapes of the trees, being CC usually estimated assuming a circular shape (West, 2009). Conversely, the use of PNOA orthophotos allows determining in a simple and precise way the CC. However, the main drawback in the use of these images is their low temporal resolution (2–3 years, depending on the area), which can be complemented with the use of high spatial resolution satellite, aircraft or UAV images. Thus, photointerpretation from high spatial resolution images such as PNOA orthophotos is presented as a more suitable tool in the analysis of the evolution of tree structures than field measurements.

5. Conclusion

The effect of different sustainable agricultural management practices was evaluated by combining remote sensing indexes (NDVI and SAVI) and physiological/morphological measurement (Ψ_{stem}; trunk perimeter and canopy diameter). The main conclusions that can be derived from the present study can be summarized as follows:

- The application of a severe SDI strategy (i.e. 33 % ET_c) negatively influenced VI_s, Ψ_{stem} and tree dimensions parameters, causing reductions of 13 %, 23 %, and 14 %, respectively, in comparison to full irrigation strategy. Moderate SDI (i.e. 67 % ET_c) did not significantly affect any of the parameters analyzed;
- The presence of VC in the inter-row increased VI_s by 23–42 % (NDVI) and 19–38 % (for SAVI); and reduced trunk perimeter (by 7–8 %) and canopy diameter (by 0.34–0.37 m) when compared to BS treatment. However, Ψ_{stem} of almond trees with VC did not differ from those under BS conditions;
- VI_s exhibited accurate relationships with trunk perimeter and canopy diameter, being dependent on the soil management.

Declaration of Competing Interest

The authors declare that they have no known competing financial interests or personal relationships that could have appeared to influence the work reported in this paper.

Acknowledgments

This research was funded in the frame of the projects PRECIRIEGO RTC-2017–6365-2 financed by Agencia Estatal de Investigación with European Regional Development Fund co-funds; and the European Union H2020 project SHUI GA 773903. The research was supported also by the CajaMar Caja Rural Contract “Efficient use of water resources under climate change scenarios”. I. Buesa and J.M. Ramírez-Cuesta acknowledge the postdoctoral financial support received from Juan de la Cierva Spanish Postdoctoral Program (FJC2019–042122-I and IJC2020–043601-I, respectively). Authors acknowledge David Hortelano and José Luis Ruíz García for the help provided in the field measurements acquisition. This work represents a contribution to CSIC Thematic Interdisciplinary Platform PTI TELEDETECT.

Appendix A. Supporting information

Supplementary data associated with this article can be found in the online version at doi:10.1016/j.agee.2022.108124.

References

Abbasi Surki, A., Nazari, M., Fallah, S., Iranipour, R., Mousavi, A., 2020. The competitive effect of almond trees on light and nutrients absorption, crop growth rate, and the yield in almond–cereal agroforestry systems in semi-arid regions. Agrofor. Syst. 94, 1111–1122. https://doi.org/10.1007/s10457-019-00469-2.

Aguirre-García, S.D., Aranda-Barranco, S., Nieto, H., Serrano-Ortiz, P., Sánchez-Cañete, E.P., Guerrero-Rascado, J.L., 2021. Modelling actual evapotranspiration using a two source energy balance model with Sentinel imagery in herbaceous-free and herbaceous-cover Mediterranean olive orchards. Agric. For. Meteorol. 311, 108692.

Alganci, U., Ozdogan, M., Sertel, E., Ormeci, C., 2014. Estimating maize and cotton yield in southeastern Turkey with integrated use of satellite images, meteorological data and digital photographs. Field Crops Res. 157, 8–19. https://doi.org/10.1016/j.fcr.2013.12.006.

Almagro, M., de Vente, J., Boix-Fayos, C., García-Franco, N., Melgares de Aguilar, J., González, D., Solé-Benet, A., Martínez-Mena, M., 2016. Sustainable land management practices as providers of several ecosystem services under rainfed Mediterranean agroecosystems. Mitig. Adapt. Strateg. Glob. Change 21, 1029–1043. https://doi.org/10.1007/S11027-013-9535-2/FIGURES/4.

Arenas-Corraliza, I., Nieto, A., Moreno, G., 2020. Automatic mapping of tree crowns in scattered-tree woodlands using low-density LiDAR data and infrared imagery. Agrofor. Syst. 94, 1989–2002. https://doi.org/10.1007/S10457-020-00517-2.

Asrar, G., Fuchs, M., Kanemasu, E.T., Hatfield, J.L., 1984. Estimating absorbed photosynthetic radiation and leaf area index from spectral reflectance in wheat. Agron. J. 76, 300–306. https://doi.org/10.2134/agronj1984.00021962007600020029x.

Balbontín, C., Campos, I., Odi-Lara, M., Ibacache, A., Calera, A., 2017. Irrigation performance assessment in table grape using the reflectance-based crop coefficient. Remote Sens. https://doi.org/10.3390/rs9121276.

Baret, F., Guyot, G., 1991. Potentials and limits of vegetation indices for LAI and APAR assessment. Remote Sens. Environ. 35 (2–3), 161–173. https://doi.org/10.1016/0034-4257(91)90009-U.

Bausch, W.C., Neale, C.M.U., 1987. Crop coefficients derived from reflected canopy radiation: a concept. Trans. ASAE 30, 0703–0709. https://doi.org/10.13031/2013.30463.

Bellvert, J., Adeline, K., Baram, S., Pierce, L., Sanden, B.L., Smart, D.R., 2018. Monitoring crop evapotranspiration and crop coefficients over an almond and pistachio orchard throughout remote sensing. Remote Sens. 10. https://doi.org/10.3390/rs10122001.

Bellvert, J., Nieto, H., Pelechá, A., Jofre-Čekalović, C., Zazurca, L., Miarnau, X., 2021. Remote sensing energy balance model for the assessment of crop evapotranspiration and water status in an almond rootstock collection. Front. Plant Sci. 12. https://doi.org/10.3389/fpls.2021.608967.

Borlaf-Mena, I., Tanase, M.A., Gómez-Sal, A., 2019. Methods for tree cover extraction from high resolution orthophotos and airborne LiDAR scanning in Spanish dehesas. Rev. De. Teledetec. 2019, 17–32. https://doi.org/10.4995/raet.2019.11320.

Burchard-Levine, V., Nieto, H., Riaño, D., Migliavacca, M., El-Madany, T.S., Guzinski, R., Carrara, A., Martín, M.P., 2021. The effect of pixel heterogeneity for remote sensing based retrievals of evapotranspiration in a semi-arid tree-grass ecosystem. Remote Sens. Environ. 260, 112440.

Calera, A., Campos, I., Osann, A., D'Urso, G., Menenti, M., 2017. Remote sensing for crop water management: from ET modelling to services for the end users. Sens. (Switz.). https://doi.org/10.3390/s17051104.

Campos, I., Neale, C.M.U., Calera, A., Balbontín, C., González-Piqueras, J., 2010. Assessing satellite-based basal crop coefficients for irrigated grapes (Vitis vinifera L.). Agric. Water Manag. 98, 45–54. https://doi.org/10.1016/j.agwat.2010.07.011.

Chemura, A., van Duren, I., van Leeuwen, L.M., 2015. Determination of the age of oil palm from crown projection area detected from WorldView-2 multispectral remote sensing data: The case of Ejisu-Juaben district, Ghana. ISPRS J. Photogramm. Remote Sens. 100, 118–127. https://doi.org/10.1016/j.isprsjprs.2014.07.013.

Choudhury, B.J., Ahmed, N.U., Idso, S.B., Reginato, R.J., Daughtry, C.S.T., 1994. Relations between evaporation coefficients and vegetation indices studied by model simulations. Remote Sens. Environ. 50, 1–17. https://doi.org/10.1016/0034-4257(94)90090-6.

Conesa, M.R., Conejero, W., Vera, J., Ramírez-Cuesta, J.M., Ruiz-Sánchez, M.C., 2019. Terrestrial and remote indexes to assess moderate deficit irrigation in early-maturing nectarine trees. Agronomy 9, 630. https://doi.org/10.3390/agronomy9100630.

Congedo, L., 2021. Semi-automatic classification plugin: a python tool for the download and processing of remote sensing images in QGIS. J. Open Source Softw. 6 (64), 3172. https://doi.org/10.21105/joss.03172.

De Leijster, V., Verburg, R.W., Santos, M.J., Wassen, M.J., Martínez-Mena, M., de Vente, J., Verweij, P.A., 2020. Almond farm profitability under agroecological management in south-eastern Spain: Accounting for externalities and opportunity costs. Agric. Syst. 183, 102878 https://doi.org/10.1016/j.agsy.2020.102878.

Delgado, J.A., Nearing, M.A., Rice, C.W., 2013. Conservation practices for climate change adaptation. In: Advances in Agronomy. Academic Press, pp. 47–115. https://doi.org/10.1016/B978-0-12-407685-3.00002-5.

Díaz-Varela, R.A., De La Rosa, R., León, L., Zarco-Tejada, P.J., Lucieer, A., Rascher, U., Bareth, G., Baghdadi, N., Thenkabail, P.S., 2015. High-resolution airborne UAV imagery to assess olive tree crown parameters using 3d photo reconstruction: application in breeding trials. Remote Sens. 2015 Vol. 7, 4213–4232. https://doi.org/10.3390/RS70404213.

Duchemin, B., Hadria, R., Erraki, S., Boulet, G., Maisongrande, P., Chehbouni, A., Escadafal, R., Ezzahar, J., Hoedjes, J.C.B., Kharrou, M.H., Khabba, S., Mougenot, B., Olioso, A., Rodriguez, J.C., Simonneaux, V., 2006. Monitoring wheat phenology and irrigation in Central Morocco: on the use of relationships between evapotranspiration, crops coefficients, leaf area index and remotely-sensed vegetation indices. Agric. Water Manag. 79, 1–27. https://doi.org/10.1016/j.agwat.2005.02.013.

Eekhout, J.P.C., de Vente, J., 2019. Assessing the effectiveness of sustainable land management for large-scale climate change adaptation. Sci. Total Environ. 654, 85–93. https://doi.org/10.1016/J.SCITOTENV.2018.10.350.

Egea, G., Dodd, I.C., Gonzalez-Real, M.M., Domingo, R., Baille, A., 2011. Partial rootzone drying improves almond tree leaf-level water use efficiency and afternoon water status compared with regulated deficit irrigation. Funct. Plant Biol. 38 (5), 372–385. https://doi.org/10.1071/FP10247.

Egea, G., Nortes, P.A., Domingo, R., Baille, A., Pérez-Pastor, A., González-Real, M.M., 2013. Almond agronomic response to long-term deficit irrigation applied since orchard establishment. Irrig. Sci. 31, 445–454. https://doi.org/10.1007/s00271-012-0322-8.

Er-Raki, S., Chehbouni, A., Guemouria, N., Duchemin, B., Ezzahar, J., Hadria, R., 2007. Combining FAO-56 model and ground-based remote sensing to estimate water consumptions of wheat crops in a semi-arid region. Agric. Water Manag. 87, 41–54. https://doi.org/10.1016/J.AGWAT.2006.02.004.

Espadafor, M., Orgaz, F., Testi, L., Lorite, I.J., Villalobos, F.J., 2015. Transpiration of young almond trees in relation to intercepted radiation. Irrig. Sci. 33, 265–275. https://doi.org/10.1007/s00271-015-0464-6.

Fereres, E., Soriano, M.A., 2007. Deficit irrigation for reducing agricultural water use. J. Exp. Bot. 147–159. https://doi.org/10.1093/jxb/erl165.

Fereres, E., Martinich, D.A., Aldrich, T.M., Castel, J.R., Holzapfel, E., Schulbach, H., 1982. Drip irrigation saves money in young almond orchards. Calif. Agric. 36, 12–13.

Fracchiolla, M., Terzi, M., Frabboni, L., Caramia, D., Lasorella, C., De Giorgio, D., Montemurro, P., Cazzato, E., 2016. Influence of different soil management practices on ground-flora vegetation in an almond orchard. Renew. Agric. Food Syst. 31, 300–308. https://doi.org/10.1017/S1742170515000241.

García-Tejero, I.F., Hernández, A., Padilla-Díaz, C.M., Diaz-Espejo, A., Fernández, J.E., 2017. Assessing plant water status in a hedgerow olive orchard from thermography at plant level. Agric. Water Manag. 188, 50–60. https://doi.org/10.1016/J.AGWAT.2017.04.004.

Girona, J., Mata, M., Marsal, J., 2005. Regulated deficit irrigation during the kernel-filling period and optimal irrigation rates in almond. Agric. Water Manag. 75 (2), 152–167. https://doi.org/10.1016/j.agwat.2004.12.008.

Glenn, E.P., Neale, C.M.U., Hunsaker, D.J., Nagler, P.L., 2011. Vegetation index-based crop coefficients to estimate evapotranspiration by remote sensing in agricultural and natural ecosystems. Hydrol. Process. 25, 4050–4062. https://doi.org/10.1002/hyp.8392.

Goldhamer, D.A., Fereres, E., 2017. Establishing an almond water production function for California using long-term yield response to variable irrigation. Irrig. Sci. 35, 169–179. https://doi.org/10.1007/s00271-016-0528-2.

González-Dugo, M.P., Mateos, L., 2008. Spectral vegetation indices for benchmarking water productivity of irrigated cotton and sugarbeet crops. Agric. Water Manag. 95, 48–58. https://doi.org/10.1016/j.agwat.2007.09.001.

González-Dugo, V., Zarco-Tejada, P.J., Intrigliolo, D.S., Ramírez-Cuesta, J.M., 2020. Normalization of the crop water stress index to assess the within-field spatial variability of water stress sensitivity. Precis. Agric. 1–20. https://doi.org/10.1007/s11119-020-09768-6.

Gutiérrez-Gordillo, S., Durán Zuazo, V.H., Hernández-Santana, V., Gil, F.F., Escalera, A. G., Amores-Agüera, J.J., García-Tejero, I.F., 2020. Cultivar dependent impact on yield and its components of young almond trees under sustained-deficit irrigation in semi-arid environments. Agronomy 10, 733. https://doi.org/10.3390/agronomy10050733.

Huete, A.R., 1988. A soil-adjusted vegetation index (SAVI. Remote Sens. Environ. 25 (3), 295–309. https://doi.org/10.1016/0034-4257(88)90106-X.

Hunsaker, D.J., Pinter, P.J., Barnes, E.M., Kimball, B.A., 2003. Estimating cotton evapotranspiration crop coefficients with a multispectral vegetation index. Irrig. Sci. 22, 95–104. https://doi.org/10.1007/s00271-003-0074-6.

Hunsaker, D.J., Pinter, P.J., Kimball, B.A., 2005. Wheat basal crop coefficients determined by normalized difference vegetation index. Irrig. Sci. 24, 1–14. https://doi.org/10.1007/s00271-005-0001-0.

Jiménez-Brenes, F.M., López-Granados, F., Castro, A.I., Torres-Sánchez, J., Serrano, N., Peña, J.M., 2017. Quantifying pruning impacts on olive tree architecture and annual canopy growth by using UAV-based 3D modelling. Plant Methods 13, 1–15. https://doi.org/10.1186/S13007-017-0205-3/FIGURES/13.

Johansen, K., Duan, Q., Tu, Y.H., Searle, C., Wu, D., Phinn, S., Robson, A., McCabe, M.F., 2020. Mapping the condition of macadamia tree crops using multi-spectral UAV and WorldView-3 imagery. ISPRS J. Photogramm. Remote Sens. 165, 28–40. https://doi.org/10.1016/J.ISPRSJPRS.2020.04.017.

Khaliq, A., Comba, L., Biglia, A., Aimonino, D.R., Chiaberge, M., Gay, P., 2019. Comparison of satellite and UAV-based multispectral imagery for vineyard variability assessment. Remote Sens. 11. https://doi.org/10.3390/rs11040436.

Lal, R., 2013. Enhancing ecosystem services with no-till. Renew. Agric. Food Syst. 28, 102–114. https://doi.org/10.1017/S1742170512000452.

Liu, R., Thomas, B.W., Shi, X., Zhang, X., Wang, Z., Zhang, Y., 2021. Effects of ground cover management on improving water and soil conservation in tree crop systems: A meta-analysis. Catena 199, 105085. https://doi.org/10.1016/J.CATENA.2020.105085.

Martínez-Mena, M., Boix-Fayos, C., Carrillo-López, E., Díaz-Pereira, E., Zornoza, R., Sánchez-Navarro, V., Acosta, J.A., Martínez-Martínez, S., Almagro, M., 2021a. Short-term impact of crop diversification on soil carbon fluxes and balance in rainfed and irrigated woody cropping systems under semiarid Mediterranean conditions. Plant Soil 467, 499–514. https://doi.org/10.1007/S11104-021-05101-W/FIGURES/3.

Martínez-Mena, M., Perez, M., Almagro, M., Garcia-Franco, N., Díaz-Pereira, E., 2021b. Long-term effects of sustainable management practices on soil properties and crop yields in rainfed Mediterranean almond agroecosystems. Eur. J. Agron. 123, 126207 https://doi.org/10.1016/j.eja.2020.126207.

Mateos, L., González-Dugo, M.P., Testi, L., Villalobos, F.J., 2013. Monitoring evapotranspiration of irrigated crops using crop coefficients derived from time series of satellite images. I. Method validation. Agric. Water Manag. 125, 81–91. https://doi.org/10.1016/j.agwat.2012.11.005.

Milgroom, J., Soriano, M.A., Garrido, J.M., Gómez, J.A., Fereres, E., 2007. The influence of a shift from conventional to organic olive farming on soil management and erosion risk in southern Spain. Renew. Agric. Food Syst. 22, 1–10. https://doi.org/10.1017/S1742170507001500.

Moldero, D., López-Bernal, Á., Testi, L., Lorite, I.J., Fereres, E., Orgaz, F., 2021. Long-term almond yield response to deficit irrigation. Irrig. Sci. 1, 3. https://doi.org/10.1007/s00271-021-00720-8.

Morugán-Coronado, A., Linares, C., Gómez-López, M.D., Faz, Á., Zornoza, R., 2020. The impact of intercropping, tillage and fertilizer type on soil and crop yield in fruit orchards under Mediterranean conditions: A meta-analysis of field studies. Agric. Syst. https://doi.org/10.1016/j.agsy.2019.102736.

Ozdemir, I., 2008. Estimating stem volume by tree crown area and tree shadow area extracted from pan-sharpened Quickbird imagery in open Crimean juniper forests. Int. J. Remote Sens. 29, 5643–5655. https://doi.org/10.1080/01431160802082155.

Pinter, P.J., Hatfield, J.L., Schepers, J.S., Barnes, E.M., Moran, M.S., Daughtry, C.S.T., Upchurch, D.R., 2003. Remote sensing for crop management. Photogramm. Eng. Remote Sens. 69, 647–664. https://doi.org/10.14358/PERS.69.6.647.

Pôças, I., Paço, T.A., Paredes, P., Cunha, M., Pereira, L.S., 2015. Estimation of actual crop coefficients using remotely sensed vegetation indices and soil water balance modelled data. Remote Sens. 2015 Vol. 7, 2373–2400. https://doi.org/10.3390/RS70302373.

Popescu, S.C., Wynne, R.H., Nelson, R.F., 2003. Measuring individual tree crown diameter with lidar and assessing its influence on estimating forest volume and biomass. Can. J. Remote Sens. 29, 564–577. https://doi.org/10.5589/m03-027.

Powlson, D.S., Gregory, P.J., Whalley, W.R., Quinton, J.N., Hopkins, D.W., Whitmore, A. P., Hirsch, P.R., Goulding, K.W.T., 2011. Soil management in relation to sustainable agriculture and ecosystem services. Food Policy 36, S72–S87. https://doi.org/10.1016/j.foodpol.2010.11.025.

Rahman, M.M., Robson, A., Bristow, M., 2018. Exploring the potential of high resolution worldview-3 Imagery for estimating yield of mango. Remote Sens. 10, 1866. https://doi.org/10.3390/rs10121866.

Ramos, M.E., Benítez, E., García, P.A., Robles, A.B., 2010. Cover crops under different managements vs. frequent tillage in almond orchards in semiarid conditions: effects on soil quality. Appl. Soil Ecol. 44, 6–14. https://doi.org/10.1016/j.apsoil.2009.08.005.

Repullo-Ruibérriz de Torres, M.A., Moreno-García, M., Ordóñez-Fernández, R., Rodríguez-Lizana, A., Cárceles Rodríguez, B., García-Tejero, I.F., Durán Zuazo, V.H., Carbonell-Bojollo, R.M., 2021. Cover crop contributions to improve the soil nitrogen and carbon sequestration in almond orchards (SW Spain). Agronomy 11, 387. https://doi.org/10.3390/agronomy11020387.

Rouse Jr, J.W., Haas, R.H., Schell, J.A., Deering, D.W., 1973. Monitoring the vernal advancement and retrogradation (green wave effect) of natural vegetation (No. NASA-CR-132982).

Sarron, J., Malézieux, É., Sané, C.A.B., Faye, É., 2018. Mango yield mapping at the orchard scale based on tree structure and land cover assessed by UAV. Remote Sens. 1900 (10), 1900. https://doi.org/10.3390/RS10121900.

Trout, T.J., Johnson, L.F., Gartung, J., 2008. Remote sensing of canopy cover in horticultural crops. HortScience 43, 333–337. https://doi.org/10.21273/hortsci.43.2.333.

Tucker, C.J., 1979. Red and photographic infrared linear combinations for monitoring vegetation. Remote Sens. Environ. 8, 127–150. https://doi.org/10.1016/0034-4257(79)90013-0.

Tucker, C.J., Holben, B.N., Elgin, J.H., McMurtrey, J.E., 1981. Remote sensing of total dry-matter accumulation in winter wheat. Remote Sens. Environ. 11, 171–189. https://doi.org/10.1016/0034-4257(81)90018-3.

Underwood, J.P., Hung, C., Whelan, B., Sukkarieh, S., 2016. Mapping almond orchard canopy volume, flowers, fruit and yield using lidar and vision sensors. Comput. Electron. Agric. 130, 83–96. https://doi.org/10.1016/J.COMPAG.2016.09.014.

Verma, N.K., Lamb, D.W., Reid, N., Wilson, B., 2016. Comparison of canopy volume measurements of scattered eucalypt farm trees derived from high spatial resolution imagery and LiDAR. Remote Sens. 8, 388. https://doi.org/10.3390/rs8050388.

Vicente-Vicente, J.L., García-Ruiz, R., Francaviglia, R., Aguilera, E., Smith, P., 2016. Soil carbon sequestration rates under Mediterranean woody crops using recommended management practices: A meta-analysis. Agric., Ecosyst. Environ. 235, 204–214. https://doi.org/10.1016/J.AGEE.2016.10.024.

Wagner, F.H., Ferreira, M.P., Sanchez, A., Hirye, M.C.M., Zortea, M., Gloor, E., Phillips, O.L., de Souza Filho, C.R., Shimabukuro, Y.E., Aragão, L.E.O.C., 2018. Individual tree crown delineation in a highly diverse tropical forest using very high resolution satellite images. ISPRS J. Photogramm. Remote Sens. 145, 362–377. https://doi.org/10.1016/J.ISPRSJPRS.2018.09.013.

Wang, K., Zhou, J., Zhang, W., Zhang, B., 2021. Mobile LiDAR scanning system combined with canopy morphology extracting methods for tree crown parameters evaluation in orchards. Sensors 2021 21 (2), 339. https://doi.org/10.3390/S21020339.

West, P.W., 2009. Tree and forest measurement. Tree and Forest Measurement, second ed. Springer, Berlin Heidelberg. https://doi.org/10.1007/978-3-540-95966-3.

Wezel, A., Casagrande, M., Celette, F., Vian, J.F., Ferrer, A., Peigné, J., 2014. Agroecological practices for sustainable agriculture. A review. Agron. Sustain. Dev. 34 (1), 1–20. https://doi.org/10.1007/s13593-013-0180-7.

Whiteside, T., Ahmad, W., 2008. Estimating canopy cover from eucalypt dominant tropical savanna using the extraction of tree crowns from very high resolution imagery. Proceedings of GEOBIA 2008 - Pixels, Objects, Intelligence: GEOgraphic Object-Based Image Analysis for the 21st Century, Calgary, 6–7 August 2008.

Xue, J., Su, B., 2017. Significant remote sensing vegetation indices: a review of developments and applications. J. Sens. 2017. https://doi.org/10.1155/2017/1353691.

Zarate-Valdez, J.L., Whiting, M.L., Lampinen, B.D., Metcalf, S., Ustin, S.L., Brown, P.H., 2012. Prediction of leaf area index in almonds by vegetation indexes. Comput. Electron. Agric. 85, 24–32.

Zarco-Tejada, P.J., González-Dugo, V., Berni, J.A.J., 2012. Fluorescence, temperature and narrow-band indices acquired from a UAV platform for water stress detection using a micro-hyperspectral imager and a thermal camera. Remote Sens. Environ. 117, 322–337. https://doi.org/10.1016/J.RSE.2011.10.007.